Enabling Magnetic Beamforming in MIMO Wireless Power Transfer Using Reconfigurable Metasurface

Zhangyu Li and Zhi Sun
Department of Electrical Engineering, University at Buffalo, State University of New York, Buffalo, NY 14260
E-mail: {zhangyul, zhisun}@buffalo.edu.

GLOBECOM 2020 - 2020 IEEE Global Communications Conference | 978-1-7281-8298-8/20/$31.00 ©2020 IEEE | DOI: 10.1109/GLOBECOM42002.2020.9322096

***Abstract*—Wireless power transfer (WPT) has been widely used in IoT applications, such as mobile device charging, biomedical implants communication, and RFID field. Maximizing the power transfer efficiency (PTE) becomes one of the most crucial problems for designing the WPT systems. Magnetic induction (MI) beamforming has been proposed recently to maximize the PTE for the near field MIMO WPT systems. However, conventional magnetic beamforming in WPT systems usually requires accurate magnetic channel estimation, both amplitude and phase control of the charging source, which can not be achieved in an extreme environment. In this paper, we propose a novel magnetic induction beamforming scheme in MIMO WPT system using a reconfigurable metasurface. Instead of controlling the source currents or voltages, the reconfigurable metasurface can achieve near field beamforming only by varying the capacitor and resistance in specific coil array units. The beamforming is modeled as a discrete optimization problem and solved by using the Simulate Anneal (SA) method. Through the analytical and COMSOL simulation results, our proposed beamforming scheme can achieve approximately two times PTE of the conventional beamforming method in a 40 cm charging distance.**

I. Introduction

Recently, near field wireless power transfer (WPT) has been widely used in the mobile device and sensor nodes charging in communication networks. Magnetic resonant coupling wireless power transfer (MRC-WPT) is one of the most popular configurations, which utilizes the mutual coupling of TX and RX to deliver the power. However, when the charging distance increases, or the position of the RX is not aligned, the coupling effect is weakened, which causes low power transfer efficiency.

Thus, maximizing the achievable power transfer efficiency in dynamic WPT scenarios becomes one of the key issues in the WPT systems design. In [5], it proves that a PTE upper bound of 50 % can be achieved by conjugate impedance matching on the TX and RX sides. Work done in [2] shows that a theoretically 100% PTE can be realized through optimal load design when the charging distance is close enough. However, these works do not address the problem of low PTE brought by the varying of charging position and distance. A Magnetic MIMO technique is proposed in [6], the amplitude and phase of the source currents are manipulated to achieve magnetic beamforming for MIMO WPT system, the experimental results show that the overall charging time is shortened by increasing the PTE. Work done in [4] gives specific TX current optimization schemes

This work was supported by the US National Science Foundation (NSF) under Grant No. 1652502.

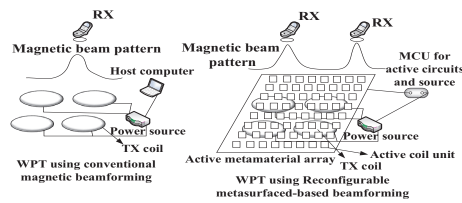

Fig. 1. System architecture of wireless power transfer using reconfigurable metasurface-based beamforming vs. conventional magnetic beamforming.

to maximize the PTE in the Magnetic MIMO system. These magnetic MIMO schemes give the optimal WPT solution when the RX is on a particular position, but the systems need accurate magnetic channel estimation and control of current in the charging source, which can not be realized when the charging source is unchangeable or can not be manipulated in extreme environments. Besides, the long-distance PTE is still low due to significant path loss. Passive metasurface enhanced WPT in [3] shows that a high PTE is obtained within a 2 m range in a point-to-point power transfer case. However, the directions and positions of power TX and RX are constrained strictly. Nowadays, in those extreme WPT scenarios, none of the existing WPT schemes can satisfy all the dynamic requirements: (1) Maximum PTE is desired. (2) The configuration of the power source can not be manipulated. (3) The host can not communicate with the RX to acquire the channel information.

In this paper, we propose a magnetic induction beamforming scheme using reconfigurable metasurface, which can improve the PTE of the MIMO wireless power transfer system in dynamic scenarios. As shown in Fig. 1, we use a reconfigurable metasurface to complete the magnetic beamforming process instead of manipulating the TXs in conventional magnetic beamforming. The reconfigurable metasurface is consist of an active metamaterial layer, which is settled above the power source, and the MCU controls the active circuits. Inspired by our work in [7], the non-foster active circuit is used to obtain negative resistance and capacitor to control each coil unit on the metamaterial layer. In order to achieve the magnetic beamforming, when the receiver is in power receiving mode, the MCU measures the current in each TX to process the magnetic channel estimation, while the voltage of each TX is fixed. After the channel estimation, the MCU knows the receivers' position and runs the algorithm to derive the optimal circuit parameter configuration of each unit in the active metasurface. Then the magnetic beamforming is done through MCU varying the

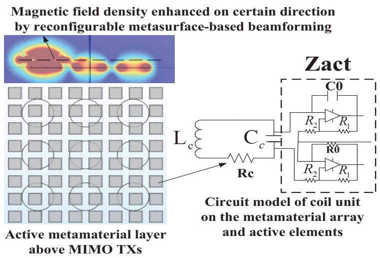

Fig. 2. The topology of active metamaterial beamforming layer with the circuit model of coil unit on the array and active elements.

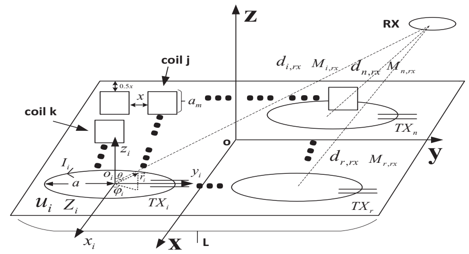

Fig. 3. Magnetic channel model of reconfigurable metasurface-based MIMO wireless power transfer system.

impedance profile of the metamaterial layer. Our reconfigurable metasurface-based beamforming scheme does not need to manipulate the power source, which makes our system workable in extreme WPT scenarios. Besides, we only use the MCU instead of the host computer in the conventional beamforming system, which reduces the cost. Through the analytical and simulation results, the proposed magnetic induction beamforming scheme can achieve two times the PTE of the conventional magnetic beamforming scheme in a 40 cm charging distance.

The remainder of the paper is organized as follows. The architecture of the reconfigurable metasurface-based magnetic beamforming system is introduced in Section II. Then the circuit and channel model, including the beamforming protocol, are analyzed in Section III. The formulation of the beamforming problem and solution are presented in Section IV. The analytical and COMSOL simulation results are evaluated in Section V. Section VI concludes the paper.

II. Reconfigurable Metasurface-based Magnetic Beamforming System Architecture

The system architecture of the proposed reconfigurable metasurface-based magnetic beamforming system is shown in Fig. 1. The conventional magnetic beamforming scheme for WPT requires the host computer to manipulate the current distribution in different TXs. Meanwhile, the RX needs to communicate with the host computer for magnetic channel estimation [4]. The idea of our reconfigurable metasurface-based beamforming scheme is different from conventional magnetic beamforming. We are using an active metamaterial array, which consists of coil units with active circuits. The metamaterial layer is put above the MIMO WPT TXs and connected to the MCU. The MCU does not need to control the current on each TX or communicate with RXs. Instead, the MCU is used to vary the parameter profiles in active circuits and measure the current in each TX for magnetic beamforming.

Metasurface is proved to be effective for improving the PTE in [3]. And work done in [8] gives a magnetic beam focusing solution in the sub-wavelength scale to concentrate the magnetic field in a particular direction. Our works in [7] [9] prove that magnetic metamaterial can be manipulated through active circuits. And dynamic magnetic gain can be obtained through active metamaterial. Inspired by those works, we design a reconfigurable metasurface-based magnetic beamforming system that can focus the magnetic field generated by TXs in certain directions. The reconfigurable metasurface is consist of an active metamaterial layer and the MCU. The metamaterial layer, which consists of a number of m identical square coils, is settled between the MIMO power TXs and the RXs, as shown in Fig. 2. . The coil unit is a transfer model of the split resonant ring (SSR) and is modeled as a resistance R_c, capacity C_c, and inductance L_c in series. Since the beamforming process requires varying the impedance value of each coil unit, the active circuits are introduced. One active impedance circuit consists of fixed resistance R_0, capacitor C_0, two adjustable resistances R_1 and R_2, and two ideal operation amplifiers. The total active impedance is $Z_{act} = -\frac{R_2}{R_1}R_0 + \frac{jR_1}{\omega R_2 C_0}$, which contains an negative resistance and negative capacitor. Then the total impedance of the coil unit after applying the active element is $Z_c = R_c + j\omega L_c - \frac{j}{\omega C_c} + Z_{act}$, which can be controlled by varying the resistance R_1 and R_2 through the MCU. The magnetic beam can be steered by configuring different impedance values on each coil unit, as shown in Fig. 2, the magnetic field intensity is enhanced in a particular direction through beamforming.

Before the MCU varying the active circuits to achieve the beamforming process, it needs to know the exact position of each RX. Thus, a magnetic channel estimation scheme is needed and is presented in section III.

III. Analytical Model of Reconfigurable Metasurface-based Beamforming

In this section, the circuit and channel models of reconfigurable metasurface-based MIMO WPT system are analyzed, and the channel estimation scheme with the beamforming protocol is presented. In the following of the paper, $\hat{H}$ denotes the vector form of a magnetic field. And $\hat{H} = H \cdot \hat{s}$, where H is the amplitude of $\hat{H}$, $\hat{s}$ is a unit vector in the direction of $\hat{H}$. We use boldface letters to represent vectors and matrices.

A. Circuit and Channel Model of Reconfigurable Metasurface-based Beamforming in MIMO WPT System

Since the mutual coupling between each RX is often weak, we ignore the mutual induction between RXs. The illustration of the magnetic channel model of a reconfigurable metasurface-based MIMO wireless power transfer system is shown in Fig. 3. We do not need to control the current or voltage on the power TXs' side. Thus, the configuration of the TXs is fixed. Each power TX is modeled as an RLC resonant coil circuit. We consider that there are n TXs with identical radius a and impedance $Z_i = R + j\omega L_0 - \frac{j}{\omega C}$, where R, L_0, C are the intrinsic resistance, inductance, and capacitor of each TX. The feeding voltage is set as $u_i = u$. For the active metamaterial layer, we consider there are m (m is a perfect square) square coil units on the horizontal square board with a side length L. The coil units are uniformly distributed on the board. The side length of each square coil unit is a_m, and the distance between each coil unit is x. The distance of units on the outermost to the board margin is $0.5x$. Each coil unit is connected to the active circuit. We first analyze the case with only one RX, at power TX_i $(1 \le i \le n)$, we have:

$$I_i Z_i = u_i - j\omega \sum_{r=1, r\neq i}^{n} M_{ri} I_r - j\omega \sum_{j=1}^{m} M_{ij} I_j - j\omega M_{i,rx} I_{rx}, \qquad (1)$$

where I_i and I_r are the currents in TX_i and TX_r, I_j and I_{rx} are the currents in $coil_j$ $(1 \le j \le m)$ and RX. Z_i is the total impedance in TX_i, ω is the frequency used for wireless power transfer. It should be noticed that the j in front of ω always means imaginary unit in this paper, which is different form index j in summation terms. M_{ri}, M_{ij} and $M_{i,rx}$ are the mutual inductance between TX i and r, between TX_i and coil unit j, between TX_i and RX, respectively. At coil unit j $(1 \le j \le m)$, the circuit equation can be established as

$$I_j Z_j^m = -j\omega \sum_{i=1}^{n} M_{ij} I_i - j\omega \sum_{k=1, k\neq j}^{m} M_{jk} I_k - j\omega M_{j,rx} I_{rx}, \qquad (2)$$

where I_k is the current in coil unit k, M_{jk} and $M_{j,rx}$ are the mutual inductance between coil unit j and k, between coil unit j and RX, separately. Z_j is the total impedance of coin unit j, including the active impedance when the total coil units number is m. We have the total impedance of each unit $Z_j^m = R_j^m + j\omega L^m + \frac{1}{j\omega C_j}$, where $R_j^m = R_m + R_{act}^j$, $C_j = C_c + C_{act}^j$. Since the total number of coil units on active metamaterial layer (m) can be varied, the intrinsic resistance (R_m) and inductance (L_m) of coil m will be determined by m [7]. C_c is the compensate capacitor used for resonating at charging frequency. The active resistance and capacitance parts in coil unit j are R_{act}^j and C_{act}^j, which is controlled by the MCU.

The induced current in a particular coil j is caused by the mutual coupling from the TXs, all the other coil units on coil array, and RX. In order to analyze the essence of magnetic beamforming, we connect the circuit model with the magnetic channel model using mutual inductance. Since the induced current is caused by the magnetic flux that passing through the effective area of the coil, We have

$$\begin{cases} j\omega S_j \mu_0 H_{z,j} = j\omega \sum_{i=1}^{n} M_{ij} I_i \\ j\omega S_j \mu_0 H_{z,m}^j = j\omega \sum_{k=1, k\neq j}^{m} M_{jk} I_k, \end{cases} \qquad (3)$$

where S_j is the effective area of coil unit j, μ_0 is the permeability in the vacuum environment. $H_{z,j} \cdot \hat{z}$ is the magnetic field in z direction at the position of coil unit j caused by all the TXs. It should be noted that the coordinate of coil unit j is in the center xyz coordinate system shown in Fig. 3. $H_{z,m}^j \cdot \hat{z}$ is the total magnetic field on coil j's position generated from the currents in all the other coil units except coil unit j. Now we analyze the magnetic field distribution of a particular TX_i since the wireless charging range is almost in near field region, the magnetic field distribution of TX_i in spherical $r_i\theta_i\phi_i$ coordinate system (shown in Fig. 3) can be expressed as [10]

$$\hat{H}_{r,i} \approx \frac{a^2 I_i \cos\theta}{2r^3} \cdot \hat{r}_i, \qquad \hat{H}_{\theta,i} \approx \frac{a^2 I_i \sin\theta}{4r^3} \cdot \hat{\theta}_i, \qquad \hat{H}_{\phi,i} = 0, \qquad (4)$$

where a is the radius of TX_i, I_i is the current in TX_i. Since $H_{z,j}$ is in xyz coordinate system, we need a coordinate transformation to derive the magnetic field distribution in xyz coordinate system, which can be written as

$$\begin{cases} \hat{H}_{x,i} = [\frac{a^2 I_i \cos\theta}{2r^3} \cdot \sin\theta\cos\phi + \frac{a^2 I_i \sin\theta}{4r^3} \cdot \cos\theta\cos\phi]\hat{x}_i \\ \hat{H}_{y,i} = [\frac{a^2 I_i \cos\theta}{2r^3} \cdot \sin\theta\sin\phi + \frac{a^2 I_i \sin\theta}{4r^3} \cdot \cos\theta\sin\phi]\hat{y}_i \\ \hat{H}_{z,i} = [\frac{a^2 I_i \cos^2\theta}{2r^3} - \frac{a^2 I_i \sin^2\theta}{4r^3}]\hat{z}_i, \end{cases} \qquad (5)$$

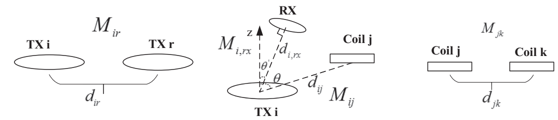

Fig. 4. Mutual induction in 3 scenarios: between TXs, between TX and RX or the coil unit on metamaterial array, between two coil units on the coil array.

where $\hat{H}_{x,i}$, $\hat{H}_{y,i}$, and $\hat{H}_{z,i}$ are the magnetic field component in direction x_i, y_i, and z_i, separately. For different TX_i, the magnetic field is expressed in the different coordinate system $(x_i y_i z_i)$. Thus, in order to calculate the summation of each $\hat{H}_{z,i}$, we need transfer each component $\hat{H}_{z,i}$ to the center xyz coordinate system in Fig. 3. The magnetic component generated by each TX after transformation is $\hat{H}_{z,i}^o$. We have

$$\hat{H}_{z,j} = \sum_{i=1}^{n} \hat{H}_{z,i}^o. \qquad (6)$$

The above deduction process can be used for calculating the magnetic field consists of any magnetic field components generated from different units (coil units, TXs or RXs) that need to be analyzed in the center xyz coordinate system.

According to equation (4), we can deduct the formula of calculating mutual inductance in different scenarios, which are shown in Fig. 4, where

$$\begin{cases} M_{ri} = \frac{\mu_0 \pi a^4}{4d_{ir}^3}, \quad (d_{ir} \text{ is the distance between TX } i \text{ and } r) \\ M_{ij} = \frac{\mu_0 a^2 a_m^2 \cos^2\theta}{2d_{ij}^3} - \frac{\mu_0 a^2 a_m^2 \sin^2\theta}{4d_{ij}^3}, \\ (d_{ij} \text{ is the distance bewtenn } TX_i \text{ and coil unit } j) \\ M_{i,rx} = \frac{\mu_0 \pi a^2 a_m^2 \cos^2\theta'}{2d_{i,rx}^3}, \\ (d_{i,rx} \text{ is the distance between } TX_i \text{ and RX}) \\ M_{jk} = \frac{\mu_0 a_m^4}{16d_{jk}^3}, (d_{jk} \text{ is the distance between coil } j \text{ and } k), \end{cases} \qquad (7)$$

where θ is the angle between z_i axis and the line connecting the center of TX_i and coil unit j, θ' is the angle between z_i axis and the line connecting the center of TX_i and RX. The distance between coil unit j and k can be expressed as $d_{jk} = \sqrt{p^2 + q^2}(a_m + x)$, where p and q are the units' number differences in x and y direction on horizontal plane.

B. Channel Estimation and Beamforming Protocol

Our reconfigurable metasurface-based magnetic beamforming system needs to know the position of each RX to conduct the beamforming process. Thus, the magnetic channel estimation is needed. The active metamaterial enabled magnetic beamforming protocol in MIMO WPT is shown in Fig. 5.

At the beginning of the WPT process, the switch of the active metamaterial layer is turned off, which means the TXs charge the RXs directly. It should be noticed that the configuration of TXs can not be manipulated. If there are multiple RXs in the WPT system, in each channel estimation cycle, only one RX is being charged. There will be N cycles for completing the channel estimation process of N RXs to conduct the beamforming in multiple RXs scenarios. Then, the MCU will have a knowledge of the current in each TX, I_i $(1 \le I_i \le n)$. We assume that the impedance of each RX device is known according to the mobile device model. We have

$$\begin{cases} I_i Z_i = u_i - j\omega \sum_{r=1, r\neq i}^{n} M_{ri} I_r - j\omega M_{i,rx} I_{rx} \\ j\omega \sum_{i=1}^{n} M_{i,rx} I_i = I_{rx} Z_{rx}, \end{cases} \qquad (8)$$

where I_{rx} is the current in the RX, Z_{rx} is the impedance of RX. Since Z_i and u_i are known constants, I_r are measured data, M_{ri} can be calculated using equations (7), after we vanish I_{rx} in

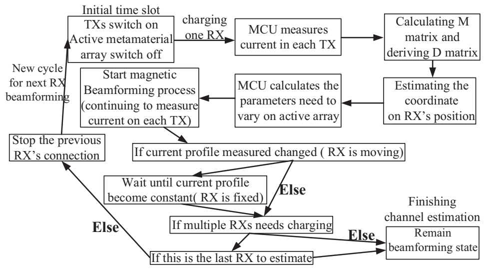

Fig. 5. The flow chart of reconfigurable metasurface beamforming protocol.

equation (8), the only unknowns in equation (8) is $M_{i,rx}$. We can establish n functions, and then we can derive $M_{i,rx}$ $(1 \leq I_i \leq n)$. The vector $\mathbf{M}$ is written in $\mathbf{M} = [M_{1,rx}, M_{2,rx}, ..., M_{n,rx}]$, we assume that the angle between the plane of Rx and horizontal plane is fixed, using equations (7), the vector $\mathbf{D}$ is derived as $\mathbf{D} = [d_{1,rx}, d_{2,rx}, ..., d_{n,rx}]$. $\mathbf{D}$ is derived based on measured data.

We can see from Fig. 3, $d_{i,rx}$ is the distance from the center of RX to TX_i. The coordinate of any TX_i in the center Cartesian coordinate system is (x_i, y_i, z_i), which is a constant when the configuration of multiple TXs is fixed, the coordinate of the center of RX is (x_{rx}, y_{rx}, z_{rx}). Let $\widetilde{d}_{i,rx} = \sqrt{(x_{rx}-x_i)^2+(y_{rx}-y_i)^2+(z_{rx}-z_i)^2}$, $\widetilde{\mathbf{D}} = [\widetilde{d}_{1,rx}, \widetilde{d}_{2,rx}, ..., \widetilde{d}_{n,rx}]$. Thus we need to estimate the coordinate value of RX's position. The estimation problem can be formulated as

$$\begin{aligned} \min_{(x_{rx}, y_{rx}, z_{rx})} \quad & \|\widetilde{\mathbf{D}} - \mathbf{D}\|^2 \\ s.t. \quad & z_{rx} \geq 0. \end{aligned} \tag{9}$$

Problem (9) is a nonlinear optimization problem, which can be solved using the steepest descent method. After we estimate the coordinate of RX, the coordinate is used in the beamforming algorithm. Then the exact impedance values of the active circuits are derived and varied through the MCU.

When the beamforming of one RX in MIMO WPT is done, the MCU still needs to monitor the current distribution in each TX. We assume all the RXs are fixed at the beginning and can move during the beamforming process, but finally, all the RXs will remain static. The beamforming towards continually moving objects are out the scope of this paper. If the current measured is each TX is changing, which means this RX is moving. We need to wait for it to stop moving, then a static current profile is observed. Then if there are multiple RXs that need to be charged, and this is not the last RX to estimate its position, we stop the connection of this RX and move to a new channel estimation cycle for the next RX beamforming. Once there exist only one RX, or we have finished the position estimation for all the RXs, the beamforming state is remaining, which means the channel estimation process is finished.

In our beamforming scheme, the more TXs used in MIMO WPT system, the higher channel estimation accuracy will be achieved based on equation (9), and the time complexity will also increase. Since the MCU does not need to communicate with RXs, our channel estimation scheme is easier and much more efficient than conventional magnetic channel estimation.

IV. Optimal Reconfigurable Metasurface-based Beamforming Design

In this section, we formulate the beamforming problem and solve it by using the Simulated Annealing (SA) algorithm.

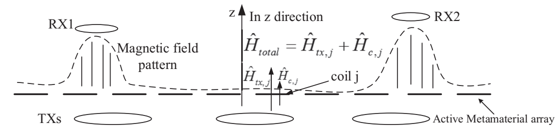

Fig. 6. The magnetic field passing through the active metamaterial layer.

A. Problem Formulation

In the MIMO WPT system, the number of coil units on the metamaterial layer is m, the number of TXs n, and the number of RXs N are fixed as constant $(n \geq 1, N \geq 1)$. Since Z_i and u_i are constant, and $Z_i = Z$, $u_i = u$. We have

$$\begin{cases} I_i Z + j\omega \sum_{r=1, r\neq i}^{n} M_{ri} I_r + j\omega \sum_{j=1}^{m} M_{ij} I_j + j\omega \sum_{s=1}^{N} M_{i,rx_s} I_{rx_s} = u \\ I_j Z_j + j\omega \sum_{k=1,k\neq j}^{m} M_{jk} I_k = -j\omega \sum_{i=1}^{n} M_{ij} I_i - j\omega \sum_{s=1}^{N} M_{j,rx_s} I_{rx_s} \\ j\omega \sum_{i=1}^{n} M_{i,rx_s} I_i + j\omega \sum_{j=1}^{m} M_{j,rx_s} I_j = I_{rx_s} Z_{rx_s}, \end{cases} \tag{10}$$

where Z_j is the impedance of active coil units and $Z_j = R_j + L_j + \frac{1}{j\omega C_j}$, M_{i,rx_s} and M_{j,rx_s} are the mutual inductance between RX_s and TX_i, coil unit j, separately. Z_{rx_s} is the impedance of RX_s, the load resistance part of Z_{rx_s} is R_{rx_s}. The PTE at RX is

$$\eta = \frac{P_{rx,R}}{P_{tx}}, \tag{11}$$

where $P_{rx,R}$ is the power received at all the loads and $P_{rx,R} = \frac{1}{2}\sum_{s=1}^{N} I_{rx_s}^2 R_{rx_s}$. P_{tx} is the source power and $P_{tx} = \frac{1}{2}\sum_{i=1}^{n} u I_i$. In equations (10), we can establish $n+m+N$ different equations. The number of unknowns are also $n+m+N$ (with n I_i's, m I_j's, and N I_{rx}'s). Once the other parameters are either calculated or measured, the PTE can be derived using equation (11).

The reconfigurable metasurface-based beamforming is achieved by varying the impedance profile (the value of Z_j on each of the coil units) of the metamaterial array through active circuits controlled by the MCU, and then calculating the maximum received power without manipulating the TXs and RXs. Thus, firstly, we need to analyze the constraints for our optimization according to the beamforming scenarios. When we adjust the impedance profile of the coil array, we can manipulate the magnetic field pattern, as shown in Fig. 6. The magnetic field generated from TXs at the coordinate of coil unit j is $\hat{H}_{tx,j}$, while the magnetic field component from all the coils on the metamaterial layer at coil unit j's coordinate is $\hat{H}_{c,j}$. After the enhancement of the active metamaterial layer, the total magnetic field in z direction can be expressed in $\hat{H}_{total} = \hat{H}_{tx,j} + \hat{H}_{c,j}$. We defined the magnetic gain brought by the active metamaterial at the position of coil j as G, where $G = \frac{H_{total}}{H_{tx,j}}$. Using equations (3) and (10), we can derive G as

$$G = \left| \frac{I_j Z_j + j\omega \sum_{s=1}^{N} M_{j,rx_s} I_{rx,s}}{I_j Z_j + j\omega \sum_{k=1,k=\neq j M_{jk} I_k}^{m} + j\omega \sum_{s=1}^{N} M_{j,rx_s} I_{rx,s}} \right|. \tag{12}$$

Unlike the symmetrical passive metamaterial array that can only generate a uniform gain, our active metamaterial layer can manipulate the distribution of the gain. Thus, we do not need large gain in the direction with no RXs. Instead, we control $G \leq \gamma_j$ (γ_j is the magnetic side-lobe gain constant at coil unit j) to reduce the magnetic side-lobe in that direction, which can be achieved by introducing active capacitance. Since when $C_j = C_c + C_{act}^j \neq C_c$ in coil units j, those units are not resonant and will not enhance the magnetic field passing through them. On those units that need to achieve large magnetic gain for beamforming, active resistance was introduced to reduce the overall resistance of coil units. A small resistance of the coil unit means less meta-loss, which can bring larger magnetic gain. In the beamforming process, the total resistance of coil unit j can be varied from $R_{min} \leq R_j \leq R_c$. The reconfigurable metasurface-based beamforming problem can be formulated as

$$
\begin{aligned}
&\max_{[\mathbf{Z_m}, \mathbf{I_n}, \mathbf{I_m}, \mathbf{I_N}]} \frac{\sum_{i=1}^{n} uI_i}{\sum_{s=1}^{N} I_{rx_s} R_{rx_s}} \\
s.t. \quad & \mathbf{M_{nn}I_n} + \mathbf{M_{nm}I_m} + \mathbf{M_{nN}I_N} = \mathbf{U_n} \\
& \mathbf{M_{mm}I_m} = -\mathbf{M_{nm}^T I_n} - \mathbf{M_{mN}I_N} \\
& \mathbf{M_{nN}^T I_n} + \mathbf{M_{mN}^T I_m} = \mathbf{U_N} \\
& R_{min} \leq R_j \leq R_c \\
& C_j = C_c \quad \text{or} \quad C_c + C_{act}^j \\
& \left| \frac{I_{j'} Z_{j'} + j\omega \sum_{s=1}^{N} M_{j',rx_s} I_{rx,s}}{I_{j'} Z_{j'} + j\omega \sum_{k=1,k\neq j'}^{m} M_{j'k} I_k + j\omega \sum_{s=1}^{N} M_{j',rx_s} I_{rx,s}} \right| \leq \gamma_{j'},
\end{aligned}
\tag{13}
$$

(j' ∈index number of coil units for reducing side lobes)

where $\mathbf{Z_m}$ is the impedance vector of coil units on active metamaterial array, $\mathbf{I_n}$, $\mathbf{I_M}$, $\mathbf{I_N}$ are the current vectors on TXs, active coil units, and RXs, separately. $\mathbf{U_n}$ is the TXs voltage vector, $\mathbf{U_N}$ is the induced voltage vector on RXs. $\mathbf{M_{nn}}$, $\mathbf{M_{nm}}$, $\mathbf{M_{nN}}$, $\mathbf{M_{mm}}$, $\mathbf{M_{mN}}$ are the mutual inductance matrices. We have

$$
\begin{aligned}
&\mathbf{Z_m} = [Z_1, Z_2, ..., Z_m]^T, \quad \mathbf{I_n} = [I_1, I_2, ...I_n]^T, \quad \mathbf{I_m} = [I_1, I_2, ...I_m]^T, \\
&\mathbf{I_N} = [I_{rx_1}, ..., I_{rx_n}]^T, \mathbf{U_n} = [u_1, ...u_n]^T, \mathbf{U_N} = [I_{rx_1} Z_{rx_1}, ..., I_{rx_1} Z_{rx_1}]^T
\end{aligned}
\tag{14}
$$

$$
\mathbf{M_{nn}} = \begin{bmatrix} Z & \cdots & j\omega M_{1n} \\ \vdots & \ddots & \vdots \\ j\omega M_{n1} & \cdots & Z \end{bmatrix}, \mathbf{M_{nm}} = \begin{bmatrix} j\omega M_{11} & \cdots & j\omega M_{1m} \\ \vdots & \ddots & \vdots \\ j\omega M_{n1} & \cdots & j\omega M_{nm} \end{bmatrix}, \tag{15}
$$

$$
\mathbf{M_{nN}} = \begin{bmatrix} j\omega M_{1,rx_1} & \cdots & j\omega M_{1,rx_N} \\ \vdots & \ddots & \vdots \\ j\omega M_{n,rx_1} & \cdots & j\omega M_{n,rx_N} \end{bmatrix}, \mathbf{M_{mm}} = \begin{bmatrix} Z_1 & \cdots & j\omega M_{1m} \\ \vdots & \ddots & \vdots \\ j\omega M_{m1} & \cdots & Z_m \end{bmatrix}, \tag{16}
$$

$$
\mathbf{M_{mN}} = \begin{bmatrix} j\omega M_{1,rx_1} & \cdots & j\omega M_{1,rx_N} \\ \vdots & \ddots & \vdots \\ j\omega M_{m,rx_1} & \cdots & j\omega M_{m,rx_N} \end{bmatrix}. \tag{17}
$$

Algorithm 1 Simulated Annealing Algorithm

```
Parameters: the index of temperature reducing time α, the maximum iteration times S, the index of iteration times β, the annealing coefficient λ (0 < λ < 1).
The initial solution Z_{α,β} the initial temperature T_α = T_0.
while T_α > End Temperature do
  for β = 0; β ≤ S do
    Randomly generate a new solution Z'_{α,β}
    if Δt = η(Z'_{α,β}) − η(Z_{α,β}) > 0 then
      η_new = η(Z'_{α,β})
    else
      if exp(Δt/T) > random[0, 1] then
        η_new = η(Z'_{α,β})
      else
        η_new = η(Z_{α,β})
      end if
    end if
    β = β + 1
  end for
  η = η_new, T_α = T_α λ, and α = α + 1
end while
```

B. Solving Beamforming Problem Using Simulated Annealing

The above problem (13) is a discrete non-linear optimization problem, which is an NP-complete (NPC) problem. In order to find an analytical solution for the problem efficiently on the computer, we use the Simulated Annealing algorithm [11].

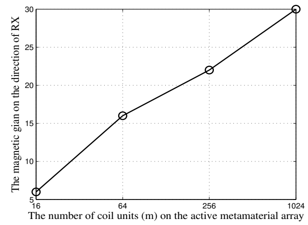

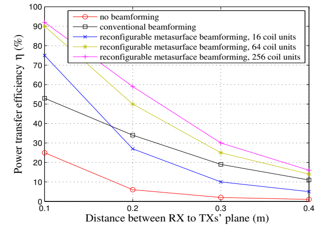

Fig. 7. Magnetic gain on beamforming direction vs. total number of coil units.

Fig. 8. Achieved PTE using SA algorithm vs. PTE using conventional beamforming and no beamforming.

The SA algorithm is presented in Algorithm 1. The solution of the objective function η is the impedance vector $\mathbf{Z}$. In the algorithm, the anneal speed is related to the maximum iteration times S, the larger the T_0 and λ are set, the more time is consumed to find a more accurate solution. The end condition is defined as the temperature is reaching a low boundary or no new solution is accepted after a certain iteration time K.

V. Analytical and Simulation results Evaluation

In this section, we evaluate the analytical beamforming performance using the SA algorithm. We use a simulation tool COMSOL Multiphysics [12] to simulate the reconfigurable metasurface-based beamforming in MIMO WPT scenario.

A. Analytical Results Evaluation

We consider there are nine identical TXs, each with a radius of 0.05 m, as shown in Fig. 2, the distance between each TX is 0.2 m. One RX with a radius of 0.02 m is set above the center of the metamaterial array. The side length of the active metamaterial board is 0.5 m. We change the total coil units number m in the metamaterial board ($m = 4, 16, 64...$). The magnetic field gain G towards the direction of RX after active metamaterial beamforming is shown in Fig. 7. When the RX and TX are fixed, the magnetic gain on the beamforming direction increases as m increases.

Then we use the SA algorithm to derive the maximum achievable PTE when m varies from 16, 64, and 256. We also compare our PTE results with the current-based magnetic beamforming results in the paper [6]. Fig. 8 shows that the PTE in no beamforming case is 25%, 6%, 2%, and 1% when the vertical distance between TX and RX are varied from 0.1 m, 0.2 m, 0.3 m, and 0.4 m, separately. While reconfigurable metasurface-based beamforming scheme (m=256) can achieve a PTE of 92%, 59%, 30%, and 16%, which is 3.68, 9.8, 15, and 16 times of the PTE without beamforming. And even compared with the complicated conventional current-controlled MIMO beamforming, we can still achieve a 1.73, 1.74, 1.58, and 1.45 times of the PTE performance, which is a significant performance improvement for MIMO WPT systems.

B. COMSOL Simulation Evaluation

In the COMSOL simulation, we fix m as 64, and nine identical TXs share the same configuration in section V-A. The model for the simulation is shown in Fig. 2. All 9 TXs are on the xy plane (z=0 m), and the active metamaterial layer is

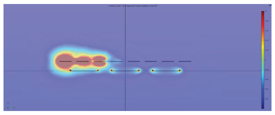

Fig. 9. Magnetic field distribution when active matematerial beamforming is used for 9 TXs and 1 RX WPT.

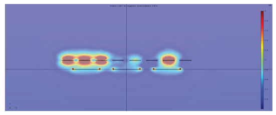

Fig. 10. Magnetic field distribution when active matematerial beamforming is used for 9 TXs and 2 RXs WPT.

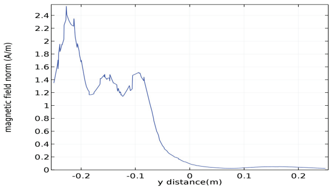

Fig. 11. The magnetic field intensity in one RX case at the line that is 0.1 m away from TXs' plane.

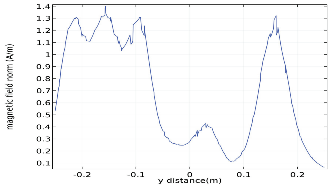

Fig. 12. The magnetic field intensity in two RXs case at the line that is 0.1 m away from TXs' plane.

parallel to all the TXs' at the plane (z=0.06 m). The length of each square coil unit is 0.02 m, the wire width is set as 2 mm. The capacitance and resistance of each coil unit can be varied through parameter settings in COMSOL, which can simulate the scenario of active array configuration after the MCU has known the optimal impedance profile for beamforming.

We consider the MIMO WPT cases with one and two RXs. In one RX case, the coordinates of RX is (x=0 m, y=-0.2 m), and we can change the coordinate z's value to simulate RX being charged in different positions. Similarly, in two RXs case, one RX is at (x=0 m, y=-0.2 m), while the other is at (x=0.125 m, y=0.125 m). We can also change the positions of two RXs in this way. The magnetic field distributions after the active magnetic beamforming are shown in Fig. 9 and 10. The magnetic field towards the direction of RX gets enhanced dramatically by the active metamaterial layer. We also plot the magnetic field intensity at the distance of 0.1 m form the TXs' plane (x=0 m, -0.25 m $\leq y \leq$ 0.25 m) in Fig. 11 and 12. The magnetic field generated by the TXs without beamforming is approximately 0.036 A/m at a 0.1 m distance from the TXs. Thus, our active metamaterial beamforming layer can successfully enhance the magnetic field in a certain direction.

The achieved PTE in the reconfigurable metasurface-based beamforming is shown in Fig. 13. We also simulate the scenario of the current-based conventional magnetic beamforming scheme for a 9×1 MIMO WPT system and compare it with our beamforming scheme. We can see that in one and two RXs scenario, our active magnetic beamforming can always achieve higher PTE than the conventional beamforming scheme and is far better than no beamforming case. When there are two RXs and the distance between TXs and RX are closer than 0.2 m, the PTE in one RX case is better than two RXs case, however, when the distance becomes larger, the PTE performance in two RXs case exceeds one RX case. At the distance of 0.4 m, our proposed beamforming can still achieve two times PTE performance of the conventional magnetic beamforming, four times of the case with no beamforming.

VI. Conclusion

In this paper, we propose an innovative reconfigurable metasurface enabled magnetic beamforming scheme that can maximize the overall PTE in the MIMO WPT system without manipulating the power source. We give the design of the active metamaterial layer. Then we analyze the circuit and channel model elaborately and present the beamforming protocol and channel estimation method. The beamforming problem is modeled as a discrete optimization problem and is solved using the simulated annealing algorithm. The analytical and simulation results show that by using our reconfigurable metasurface-based beamforming scheme, the PTE can be increased to approximately two times of using a conventional beamforming scheme. The promising result shows that our scheme can work efficiently in dynamic wireless charging scenarios that no manipulation of power source is allowed.

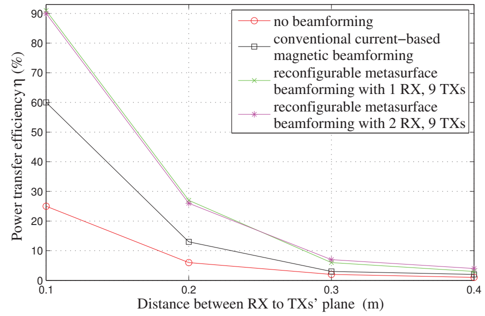

Fig. 13. Achieved PTE in the COMSOL simulation scenarios: the active metamaterial beamforming uses optimal impedance profile, compared with current-based beamforming scheme and no beamforming scheme.

References

[1] S. Hrabar, Z. Eres and J. Bartolic, "Capacitively Loaded Loop as Basic Element of Negative Permeability Meta-material," 2002 32nd European Microwave Conference, Milan, Italy, 2002, pp. 1-4.

[2] M. Zargham and P. G. Gulak,"Maximum Achievable Efficiency in Near-Field Coupled Power-Transfer Systems," in IEEE Transactions on Biomedical Circuits and Systems, vol. 6, no. 3, pp. 228-245, June 2012.

[3] H. Lang and C. D. Sarris,"Optimization of Wireless Power Transfer Systems Enhanced by Passive Elements and Metasurfaces," in IEEE Transactions on Antennas and Propagation, vol. 65, no. 10, pp. 5462-5474, Oct. 2017.

[4] G. Yang, M. R. V. Moghadam and R. Zhang,"Magnetic MIMO Signal Processing and Optimization for Wireless Power Transfer," in IEEE Transactions on Signal Processing, vol. 65, no. 11, pp. 2860-2874, 1 June1, 2017.

[5] T. Lee, The Design of CMOS Radio-Frequency Integrated Circuits, 2nd ed. Cambridge, U.K.: Cambridge Univ. Press, 2004.

[6] Jadidian, Jouya and Katabi, Dina. (2014). Magnetic MIMO: How to charge your phone in your pocket. Proceedings of the Annual International Conference on Mobile Computing and Networking, MOBICOM.

[7] Z. Li and Z. Sun,"Antenna System Optimization for Active Metamaterial-enhanced Magnetic Induction Communications," 2019 13th European Conference on Antennas and Propagation (EuCAP), Krakow, Poland, 2019, pp. 1-5.

[8] F. Gao, F. Zhang, M. Huang and D. F. Sievenpiper,"Programmable Screen for Patterning Magnetic Fields," in IEEE Transactions on Microwave Theory and Techniques, vol. 62, no. 3, pp. 481-490, March 2014.

[9] H. Guo and Z. Sun, "Full-Duplex Metamaterial-Enabled Magnetic Induction Networks in Extreme Environments," IEEE INFOCOM 2018 - IEEE Conference on Computer Communications, Honolulu, HI, 2018, pp. 558-566.

[10] C. A. Balanis, Antenna Theory. John Wiley Publishing Company, 2005.

[11] Orlin, James and Punnen, Abraham and Schulz, Andreas. Local Search in Combinatorial Optimization. Proceedings of the Fifteenth Annual ACM-SIAM Symposium on Discrete Algorithms, SODA 2004, New Orleans, Louisiana, USA, January 11-14, 2004

[12] [Online]. Avaliable: www.comsol.com.